AGU PUBLICATIONS

Geochemistry, Geophysics, Geosystems

RESEARCH ARTICLE
10.1002/2014GC005301

Key Points:
- The studied sediments contain detrital and biogenic magnetites
- No depth offset between paleomagnetic signals recorded by detrital and biogenic magnetite particles
- A significant part of the NRM is controlled by nongeomagnetic factors

Correspondence to:
T. Ouyang,
oyangtp@gig.ac.cn

Citation:
Ouyang, T., D. Heslop, A. P. Roberts, C. Tian, Z. Zhu, Y. Qiu, and X. Peng (2014), Variable remanence acquisition efficiency in sediments containing biogenic and detrital magnetites: Implications for relative paleointensity signal recording, *Geochem. Geophys. Geosyst.*, *15*, 2780–2796, doi:10.1002/2014GC005301.

Received 18 FEB 2014
Accepted 16 JUN 2014
Accepted article online 18 JUN 2014
Published online 12 JUL 2014

Variable remanence acquisition efficiency in sediments containing biogenic and detrital magnetites: Implications for relative paleointensity signal recording

Tingping Ouyang[1,2], David Heslop[2], Andrew P. Roberts[2], Chengjing Tian[1], Zhaoyu Zhu[1], Yan Qiu[3], and Xuechao Peng[3]

[1]Key Laboratory of Marginal Sea Geology, Guangzhou Institute of Geochemistry, Chinese Academy of Sciences, Guangzhou, Guangdong, China, [2]Research School of Earth Sciences, Australian National University, Canberra, Australian Capital Territory, Australia, [3]Guangzhou Marine Geological Survey, Guangzhou, Guangdong, China

Abstract Widespread geological preservation of biogenic magnetite makes it important to assess how such particles contribute to sedimentary paleomagnetic signals. We studied a sediment core from the South China Sea that passes the strict empirical criteria for magnetic "uniformity" used in relative paleointensity studies. Such assessments are based routinely on bulk magnetic parameters that often fail to enable identification of mixed magnetic mineral assemblages. Using techniques that enable component-specific magnetic mineral identification, we find that biogenic and detrital magnetites occur in approximately equal concentrations within the studied sediments. We analyzed normalized remanence signals associated with the two magnetite components to assess whether co-occurring biogenic and detrital magnetites record geomagnetic information in the same way and with the same efficiency. Paleomagnetic directions for the two components have no phase lag, which suggests that the biogenic and detrital magnetites acquired their magnetizations at equivalent times. However, we find that the biogenic magnetite is generally 2–4 times more efficient as the detrital magnetite in contributing to the natural remanent magnetization (NRM) despite their approximately equal magnetic contributions. Variations in the concentration and efficiency of remanence acquisition of the two components suggest that a significant part of the NRM is controlled by nongeomagnetic factors that will affect relative paleointensity recording. We recommend that methods suited to the detection of variable recording efficiency associated with biogenic and detrital magnetites should be used on a routine basis in relative paleointensity studies.

1. Introduction

Over the last two decades, detailed analyses of relative variations in the intensity of Earth's magnetic field have provided a previously unavailable view of the dynamic behavior of the geomagnetic field [e.g., *Valet*, 2003; *Valet et al*., 2005; *Tauxe and Yamazaki*, 2007; *Roberts et al*., 2013a]. Geomagnetic intensity variations are now used to provide a reference signal for dating sediments, often at millennial or higher resolution [e.g., *Channell et al*., 2000, 2009; *Channell and Kleiven*, 2000; *Laj et al*., 2000; *Stoner et al*., 2002; *Valet et al*., 2005; *Ziegler et al*., 2011]. An advantage of using relative paleointensity variations for dating is that they provide a geophysical signal that is independent of seawater chemistry. Relative paleointensity, therefore, is not subject to the same limitations as the marine paleoceanographic proxies that are commonly used to date marine sediments (e.g., foraminiferal $\delta^{18}O$). Nevertheless, we remain remarkably ignorant of the processes by which sediments acquire a remanent magnetization. The theoretical and empirical foundations for relative paleointensity determinations, despite the outstanding successes of such studies, are insubstantial [*Roberts et al*., 2013a].

Using sediments to estimate the ancient geomagnetic field intensity is made difficult by the fact that the magnetization of a sediment is affected by multiple variables. These variables include the strength of the ambient geomagnetic field, the magnetic mineral that records the paleomagnetic signal, magnetic mineral concentration, magnetic mineral grain size, and the mechanism by which the magnetization was acquired. The tendency of magnetic particles to flocculate with other sediment particles, such as clays, to form larger aggregates adds a floc size dependence to geomagnetic alignment efficiency that further complicates relative paleointensity determination [*Tauxe et al*., 2006; *Roberts et al*., 2013a].

Lack of a robust theoretical foundation for relative paleointensity investigations has meant that sedimentary paleointensities are estimated using an empirical approach in which the measured natural remanent magnetization (NRM) is normalized by an artificial laboratory-induced magnetization [*Levi and Banerjee*, 1976] to remove the influence of rock magnetic variations with nongeomagnetic origins. Additionally, strict rock magnetic selection criteria are imposed to help minimize rock magnetic contamination of normalized remanence records. These criteria require magnetite to be the only magnetic mineral present; it must also occur within a narrow grain size and concentration range [*King et al*., 1983; *Tauxe*, 1993]. The purpose of these criteria is to ensure that the sediment is effectively magnetically homogeneous, which limits the nongeomagnetic factors that complicate extraction of paleointensity signals. This empirical approach has been validated, for example, by the global coherence of relative paleointensity records from different environments, the consistency between paleointensity records provided by the geomagnetically modulated production of cosmogenic isotopes and those from sediments, and consistency between sedimentary paleointensity records and those obtained via inversion of high-resolution marine magnetic anomaly profiles over fast-spreading oceanic crust [*Roberts et al*., 2013a]. Nevertheless, the theoretical underpinning for relative paleointensity analysis is complicated [e.g., *Tauxe et al*., 2006]. These complications mean that we cannot determine absolute paleointensities from sediments. We, therefore, estimate relative paleointensity variations by seeking to minimize strictly the number of variables that contribute to the magnetization. For in-depth treatment of these issues, readers are referred to recent review papers [e.g., *Valet*, 2003; *Tauxe and Yamazaki*, 2007; *Roberts et al*., 2013a].

The rock magnetic parameters used to assess magnetic homogeneity of sediments in relative paleointensity studies typically reflect variations in bulk magnetic properties. They, therefore, do not enable assessment of whether a magnetic mineral assemblage under investigation contains a single magnetic grain size distribution or a more complex assemblage of magnetite particles. It has been assumed almost universally in relative paleointensity investigations that the magnetite that records the paleomagnetic signal has a detrital origin. Recent advances that enable decomposition of mixed magnetic mineral assemblages have led to much more widespread identification of biogenic magnetite in the geological record [*Roberts et al*., 2012]. In this paper, we present results from a marine sediment core that meets all of the criteria that are conventionally applied in relative paleointensity studies, but where the sedimentary magnetic mineral assemblage is principally a two-component mixture of detrital and biogenic magnetites. This provides an opportunity to assess how such magnetic mixtures affect paleomagnetic signal recording and remanence normalization in relative paleointensity studies. Such an assessment is needed if coexisting detrital and biogenic magnetites are documented more commonly in sediments.

As outlined by *Roberts et al*. [2012, 2013a, 2013b], two principal problems need to be assessed in relation to the recording of paleomagnetic signals in the presence of mixtures of detrital and biogenic magnetites. One involves the possibility of mixed remanence acquisition mechanisms. Detrital magnetic particles in sediments are typically assumed to acquire a remanent magnetization via processes associated with the depositional remanent magnetization (DRM) or postdepositional remanent magnetization (PDRM) concepts. If biogenic magnetite is produced in the water column or within the surface mixed layer of the sediment column [*Petermann and Bleil*, 1993; *Flies et al*., 2005; *Pan et al*., 2005; *Jogler et al*., 2010], it is reasonable to expect that these particles could align with the geomagnetic field through conventionally considered mechanisms associated with DRM or PDRM acquisition [*Paterson et al*., 2013; *Mao et al*., 2014]. In contrast, if magnetotactic bacteria live within the sediment below the surface mixed layer, it is possible that they will contribute to a novel biogeochemical remanent magnetization when they die [*Tarduno et al*., 1998; *Abrajevitch and Kodama*, 2009; *Larrasoaña et al*., 2014]. In this case, there ought to be a depth offset between paleomagnetic signals recorded by detrital and biogenic magnetite particles. Such offsets will complicate interpretation of paleomagnetic data and could compromise relative paleointensity determinations. The second problem is that detrital and biogenic magnetite particles will have different grain size distributions and could, therefore, be expected to respond differently to the magnetizing field [*Roberts et al*., 2012]. Assessing possible variability in recording efficiency within a single core is an important aspect of paleointensity analysis that has not been constrained before and contrasts with the more common approach of assessing the quality of a record by correlation with global or regional paleointensity stacks. In this paper, we assess these questions concerning remanence

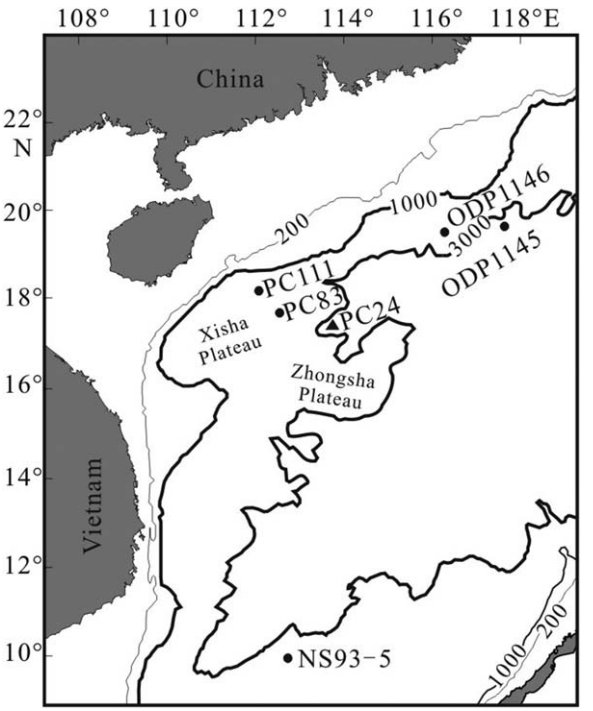

Figure 1. Map of the South China Sea, with location of the studied core (PC24) and of other cores from which relative paleointensity records have been reported. Piston cores PC83 and PC111 were studied by *Yang et al.* [2009], ODP1145 and ODP1146 were studied by *Laj et al.* [2006], and NS93-5 was studied by *Yang et al.* [2007].

acquisition mechanisms and recording efficiency for sediments whose magnetization is due to mixtures of detrital and biogenic magnetites.

2. Geological Setting and Sampling

The South China Sea (SCS) is the largest marginal sea in the northwest Pacific Ocean. The SCS can be subdivided into northwestern, southwestern, and eastern subbasins [*He and Chen*, 1987; *Liu*, 1992]. The 7.6 m long piston core (PC24) studied here was recovered by the Guangzhou Marine Geological Survey in June, 2008, from the northwestern subbasin (latitude/longitude: 17.4°N, 113.7°E) at a water depth of 3433 m (Figure 1). The recovered sediments consist of clayey silts that are yellow-gray and gray in the upper 1.01 m and gray from 1.01 to 7.6 m. Occasional fine yellow sand layers are preserved throughout the core. The yellow-gray to gray transition is likely to be a diagenetic transition. *Lyle* [1983] reported that a brown-green color transition in hemipelagic sediments is due to the iron redox boundary. We interpret the yellow-gray transition in the studied core to also represent the iron redox boundary; this interpretation is supported by the fact that the studied interval down to the base of the core contains abundant fine-grained magnetite (see below), which would not be the case if the sediments had been subjected to diagenetic sulfate reduction [*Karlin and Levi*, 1983; *Canfield and Berner*, 1987]. Paleointensity results have been frequently reported in sediments that have been subjected to iron reduction; *Yamazaki and Sølheid* [2011] argued that the iron redox boundary had no effect on recording of paleointensity signals in their studied pelagic carbonate sediments despite changes in magnetic properties across this redox front. In the core studied here, there is also a clear change in magnetic properties across this front; magnetic data from the uppermost 1 m of the core and from the yellow sandy intervals are shown below to provide contextual magnetic property information for the core, but are not included in our analysis of paleointensity signal recording. We note also that similar terrigenous continental margin gray clays have recently been demonstrated to preserve mixtures of biogenic and detrital magnetites [*Larrasoaña et al.*, 2014], which makes such sediments a useful target for assessing the effects of paleomagnetic recording in materials that contain mixtures of biogenic and detrital magnetites.

The studied core was split and one half was continuously sampled by inserting plastic cubes ($2 \times 2 \times 2$ cm^3) into the split face of core sections. Sediment at the base of each cube was then cut away with a non-magnetic knife, and the cubes were sealed with plastic end-pieces and clear polyethylene tape. In total, 380 paleomagnetic samples were taken, along with bulk sediment samples at the same depths. We attempted to extract foraminifera from the sediment to obtain a δ^{18}O record for the core, but failed because the site lies below the calcite compensation depth (CCD). The CCD is located between water depths of 3000 and 3500 m in the study area, although variable positions have been reported [*Rottman*, 1979; *Thunell et al.*, 1992; *Miao et al.*, 1994; *Wang et al.*, 1995; *Wei et al.*, 1997]. Lack of foraminiferal calcite and our inability to develop an independent age model for the studied core compromised attempts to obtain a robust relative paleointensity record that could be correlated with global or local relative paleointensity reference curves.

Instead, we focus below on assessing the relative recording efficiencies of biogenic and detrital magnetites and their implications for recording relative paleointensity signals in sediments.

3. Methods

Wide-ranging paleomagnetic and mineral magnetic measurements were made on samples from the studied PC24 sediment core. The low-field magnetic susceptibility (χ) was measured for all discrete samples using a Kappabridge MFK1-FA (AGICO) magnetic susceptibility meter at both low (976 Hz) and high (15,616 Hz) frequencies. The temperature dependence of susceptibility was measured in an argon atmosphere for representative samples from room temperature to 700°C using the Kappabridge MFK1-FA equipped with a CS-4 heating device. These measurements were made at the Guangzhou Institute of Geochemistry, Chinese Academy of Sciences. The NRM was measured and subjected to stepwise alternating field (AF) demagnetization at peak fields of 5, 10, 15, 20, 25, 30, 35, 40, 50, 60, 70, 80, and 100 mT. These measurements were performed for all discrete samples using a 2-G Enterprises 755 cryogenic magnetometer at the South China Sea Institute of Oceanology, Chinese Academy of Sciences. All other magnetic measurements were carried out at The Australian National University. An anhysteretic remanent magnetization (ARM) was imparted to all samples in a 0.05 mT direct current (DC) bias field with a superimposed 100 mT peak AF. The ARM was subsequently demagnetized at the same field steps used for NRM demagnetization. An isothermal remanent magnetization (IRM) was imparted in a 900 mT DC field, which is treated here as a saturation IRM (SIRM), using a 2-G Enterprises 760 pulse magnetizer, and was subsequently demagnetized at the same field steps used for NRM and ARM demagnetization. A 300 mT backfield was then applied to all discrete samples after imposing a new SIRM. S-ratios (S_{-300}) were calculated as $S_{-300} = (1 - IRM_{-300\ mT}/SIRM)/2$, following the definition of *Bloemendal et al*. [1992]. Hysteresis loops with a maximum applied field of 0.5 T, IRM acquisition curves with a maximum applied field of 1.0 T, backfield demagnetization curves, and low and high-resolution first-order reversal curve (FORC) diagrams were measured for tens of representative samples using a Princeton Measurements Corporation MicroMag 3900 vibrating sample magnetometer (VSM). Values of the saturation magnetization (M_s), saturation remanent magnetization (M_{rs}), and coercivity (B_c) were obtained from the hysteresis loops, while the coercivity of remanence (B_{cr}) was determined from the backfield IRM demagnetization curves. FORC diagrams were determined, with representation of the 0.05 significance levels associated with the FORC distributions, following the procedure of *Heslop and Roberts* [2012].

When estimating relative geomagnetic paleointensities, the NRM is routinely normalized with several parameters, including ARM, IRM, and χ. This simple approach has been referred to as "brute force" normalization [*Tauxe*, 1993] whereby the NRM is subjected to AF demagnetization at a certain peak field and is normalized by an ARM or IRM that has been AF demagnetized at the same peak field. Normalization by χ is considered to be less effective because (super) paramagnetic and diamagnetic minerals that do not contribute to the NRM can contribute to χ. Nevertheless, it is often used alongside other "brute force" normalizations to demonstrate that multiple normalizations yield similar results, and hence to indicate that the normalizations provide a consistent estimate of the relative geomagnetic paleointensity. We present such "brute force" normalizations below.

In contrast to "brute force" normalization, *Tauxe et al*. [1995] developed the "pseudo-Thellier" approach, which enables assessment of unwanted viscous remanence components and allows estimation of uncertainties in calculated relative paleointensities. In the "pseudo-Thellier" approach, NRM demagnetization data are plotted versus ARM acquisition data. We only measured ARM demagnetization and did not measure its acquisition. In the absence of magnetostatic interactions, ARM acquisition and demagnetization will be equivalent (for SD particles). We, therefore, plot NRM demagnetization versus ARM demagnetization data to assess signals due to the two distinct magnetite components documented in the studied core. To avoid confusion, we do not refer to this as a "pseudo-Thellier" approach, although it is essentially equivalent for SD particles when interactions are absent. A major advantage of the "pseudo-Thellier" approach is that data are plotted in a manner analogous to the "Arai" diagram [*Nagata et al*., 1963] used in absolute paleointensity studies [*Thellier and Thellier*, 1959] and that best fit slopes that relate NRM and ARM can be calculated [*Coe et al*., 1978], with estimation of the goodness of fit and optimization of the NRM/ARM slope. Biogenic and detrital magnetic particle assemblages are expected to have different coercivities. This approach, therefore, allows separation of slopes due to these components in the NRM and ARM demagnetization data, which helps to assess their relative contributions to the normalized remanence records used for relative paleointensity estimation.

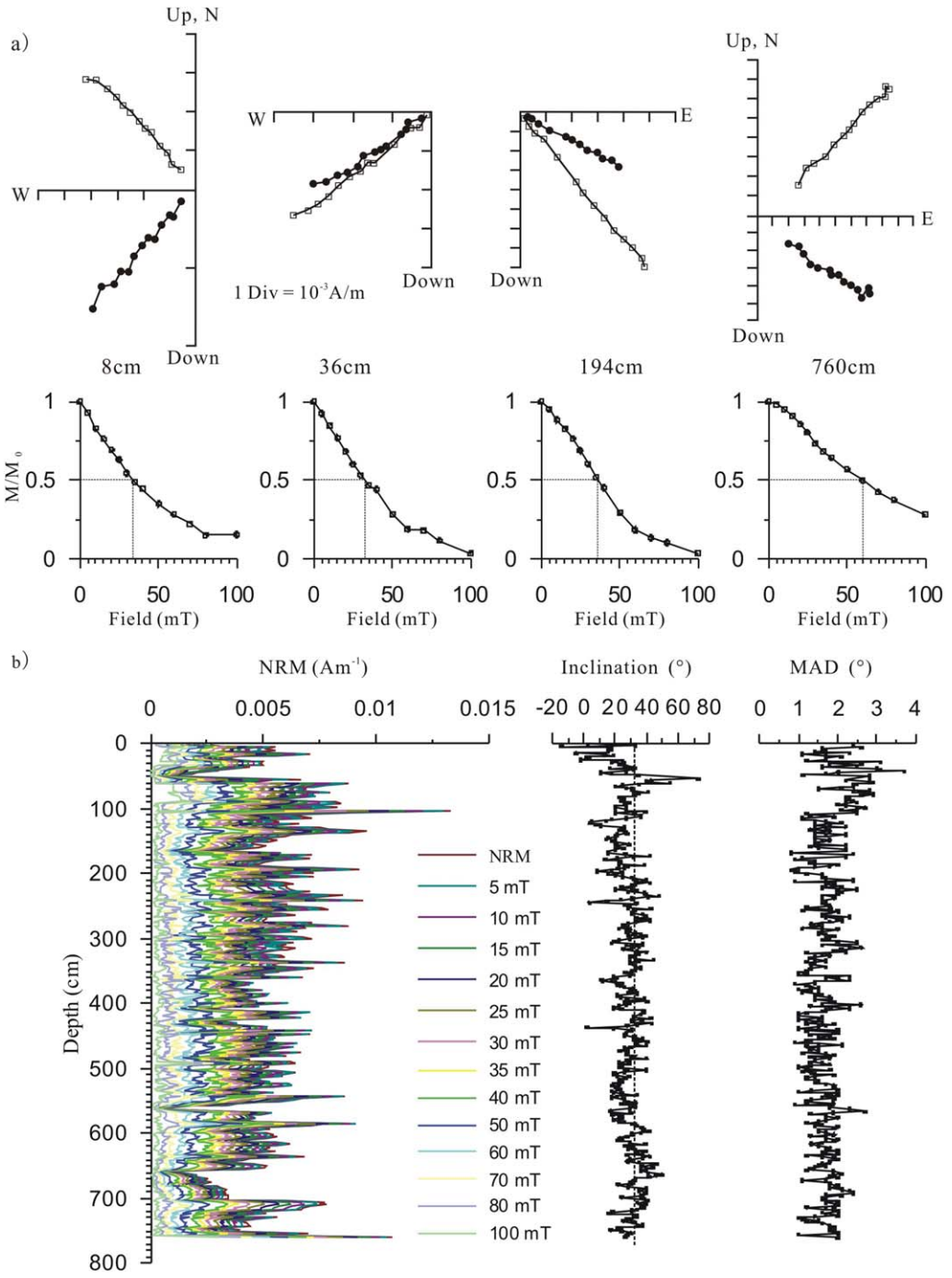

Figure 2. (a) Representative vector demagnetization diagrams and (b) down-core variations of the NRM, characteristic remanent magnetization (ChRM) inclination and maximum angular deviation (MAD) associated with the principal component analysis fit to the ChRM directions for samples from core PC24. Black circles and white squares represent projections onto the vertical and horizontal planes, respectively. The vertical dashed line indicates the expected inclination for a geocentric axial dipole field (32.1°) at the latitude of core PC24.

4. Results

Representative NRM demagnetization data are shown in Figure 2a. The NRM is almost completely demagnetized at peak fields of 100 mT for most samples, which indicates that the NRM has dominantly low coercivities. Principal component analysis was used to calculate the best fit characteristic remanent magnetization (ChRM) and maximum angular deviation (MAD) for all samples [*Kirschvink*, 1980]. ChRM

inclinations vary about an average value of 28.1°, which is close to the geocentric axial dipole field value (32.1°) expected at the site latitude (Figure 2b). MAD values are generally ~2° and are always smaller than 4° (Figure 2b), which reflects the stable nature of the ChRM (Figure 2a).

Temperature-dependent χ curves for 42 selected samples consistently reveal a major χ decrease at the Curie temperature of magnetite (Figure 3a), which indicates that magnetite is the dominant magnetic mineral within the studied sediments. For some samples, neoformation of magnetite via conversion of Fe-clay minerals is evident during heating [*Deng et al*., 2004; *Zhang et al*., 2012], which causes χ to increase above 300°C up to just below the Curie temperature of magnetite, which produces much higher χ values during cooling. Hopkinson peaks in the heating curves for some samples (e.g., at depths of 2, 532, and 752 cm) indicate the presence of single domain (SD) magnetite particles (Figure 3a). Hysteresis loops for 78 samples have the same shapes and close at or above 300 mT (Figure 3b). IRM acquisition curves also approach saturation at about 300 mT, with B_{cr} values generally less than 40 mT, although a high coercivity component is evident in some samples (Figure 3c). All of these results suggest that the main magnetic mineral(s) in the sediments have low coercivity. Fitting of components to the IRM acquisition curves reveals the presence of two low coercivity magnetic components [*Kruiver et al*., 2001] (Figure 3d). For the 78 analyzed samples, average contributions to the IRM for the two components are 50.3% and 49.6%, with average $B_{1/2}$ of 30.5 and 40.8 mT, respectively. These results indicate that the two magnetic components are due to magnetite with different grain sizes but with approximately the same concentration.

Mean B_{cr}/B_c and M_{rs}/M_s values for 78 analyzed samples are 2.42 and 0.23, respectively. The data cluster within the pseudosingle domain (PSD) field of the Day plot [*Day et al*., 1977; *Dunlop*, 2002] (Figure 3e). While such data distributions are commonly observed for sediments [e.g., *Roberts et al*., 2012], the results presented in Figure 3d indicate that the distribution must result from a mixture of magnetite with different grain sizes. Scatter in a plot of ARM susceptibility (χ_{ARM}) versus χ [*King et al*., 1982] indicates variability in the "mean" grain size of the magnetite that contributes to the bulk sediment magnetization (Figure 3f). S_{-300} values for all samples exceed 0.90, and average close to 0.95, which confirms that low coercivity magnetite dominates the magnetization of the studied sediments. χ, SIRM, and ARM, which mainly reflect magnetic mineral concentration, undergo relatively minor variations down-core, especially below the inferred iron redox front at ~1 m (Figure 4). Magnetic mineral grain-size dependent parameters (χ_{ARM}/χ, χ_{ARM}/SIRM, SIRM/χ, and the frequency dependence of susceptibility, χ_{fd}) [*Thompson and Oldfield*, 1986; *Verosub and Roberts*, 1995; *Evans and Heller*, 2003] also only undergo minor down-core variations (Figure 4). Sandy intervals at 5.60–5.65, 6.55–6.60, and 7.43–7.60 m have more variable magnetic properties and are excluded from the analysis below concerning relative paleointensity recording.

The above results indicate that the studied sediments meet the conventional criteria applied to assess the suitability of sediments for relative paleointensity investigations [*King et al*., 1983; *Tauxe*, 1993]. That is, magnetite is the dominant magnetic mineral (Figure 3; although a small high coercivity (hematite) component is indicated in some demagnetization diagrams in Figure 2a), the concentration of magnetite does not undergo large variations (Figure 4), and conventionally applied bulk magnetic measures of grain size do not reveal major variations away from an average "pseudosingle domain" grain size range (Figure 3e). However, use of magnetic techniques that allow discrimination of different grain size components, which have not been widely used in relative paleointensity investigations, reveal the likely presence of two magnetite components (Figure 3d). This is well illustrated by FORC diagrams for representative samples from different depths in the studied core, which contain mixed signatures with a central ridge signal due to magnetically noninteracting SD particles produced by magnetotactic bacteria [*Egli et al*., 2010] and an asymmetrical and vertically spread signal that diverges toward the B_u axis, which reflects the presence of coarser PSD particles within the sediments [*Roberts et al*., 2000; *Muxworthy and Dunlop*, 2002] (Figure 5). Thus, the studied sediments, which appear to be magnetically homogeneous based on the bulk magnetic parameters used in most conventional relative paleointensity studies, contain two magnetite components that are likely to respond to a magnetizing field in different ways, and will therefore record paleointensity signals differently. Such mixtures of biogenic and detrital magnetites are likely to be much more common than previously recognized in relative paleointensity studies [e.g., *Channell et al*., 2013; *Ohneiser et al*., 2013], which makes it important to understand their effects on relative paleointensity normalizations [*Roberts et al*., 2012, 2013a].

Results from three "brute force" paleointensity normalizations (NRM/χ, NRM/ARM, and NRM/IRM) are similar (Figures 6a–6c). This is often reported to be the case for sediments that pass the conventional criteria for

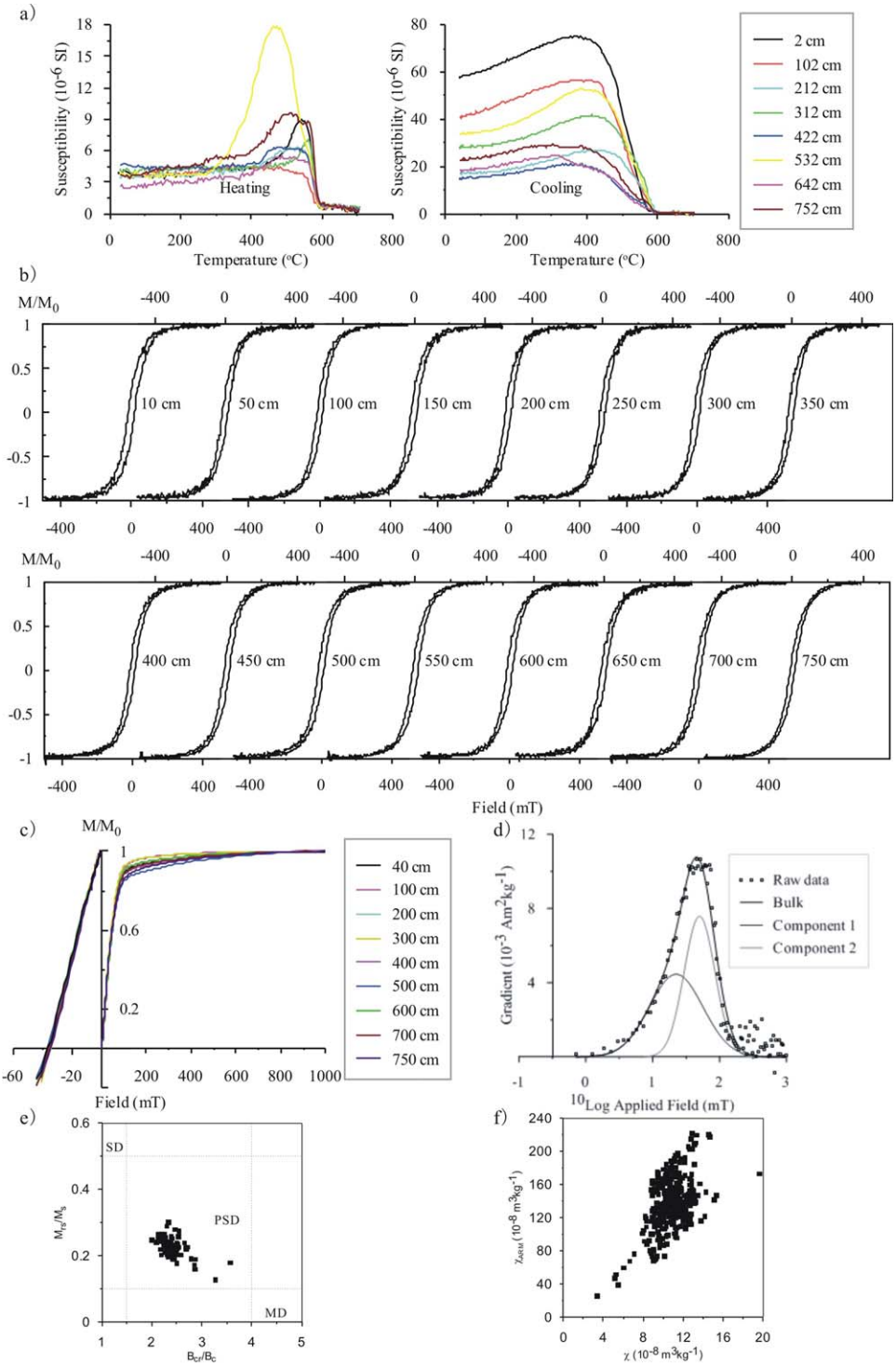

Figure 3. Mineral magnetic properties for sediments from core PC24. Representative (a) χ-T curves, (b) hysteresis loops, (c) IRM acquisition and backfield demagnetization curves, and (d) gradient acquisition plot (GAP) of IRM acquisition curves. The GAP is decomposed into two components due to detrital (magnetically softer, wide dispersion; component 1) and biogenic (magnetically harder, narrow dispersion; component 2) magnetite. (e) Day plot (after *Day et al.* [1977]) for 78 analyzed samples (SD = single domain, PSD = pseudosingle domain, and MD = multidomain), and (f) χ_{ARM} versus χ plot (after *King et al.* [1982]) for all samples.

relative paleointensity studies. However, as demonstrated above, the IRM of the studied sediments has approximately equal contributions from detrital and biogenic magnetites (Figure 3d). This provides an opportunity to assess whether the two identified magnetite components respond to the geomagnetic field

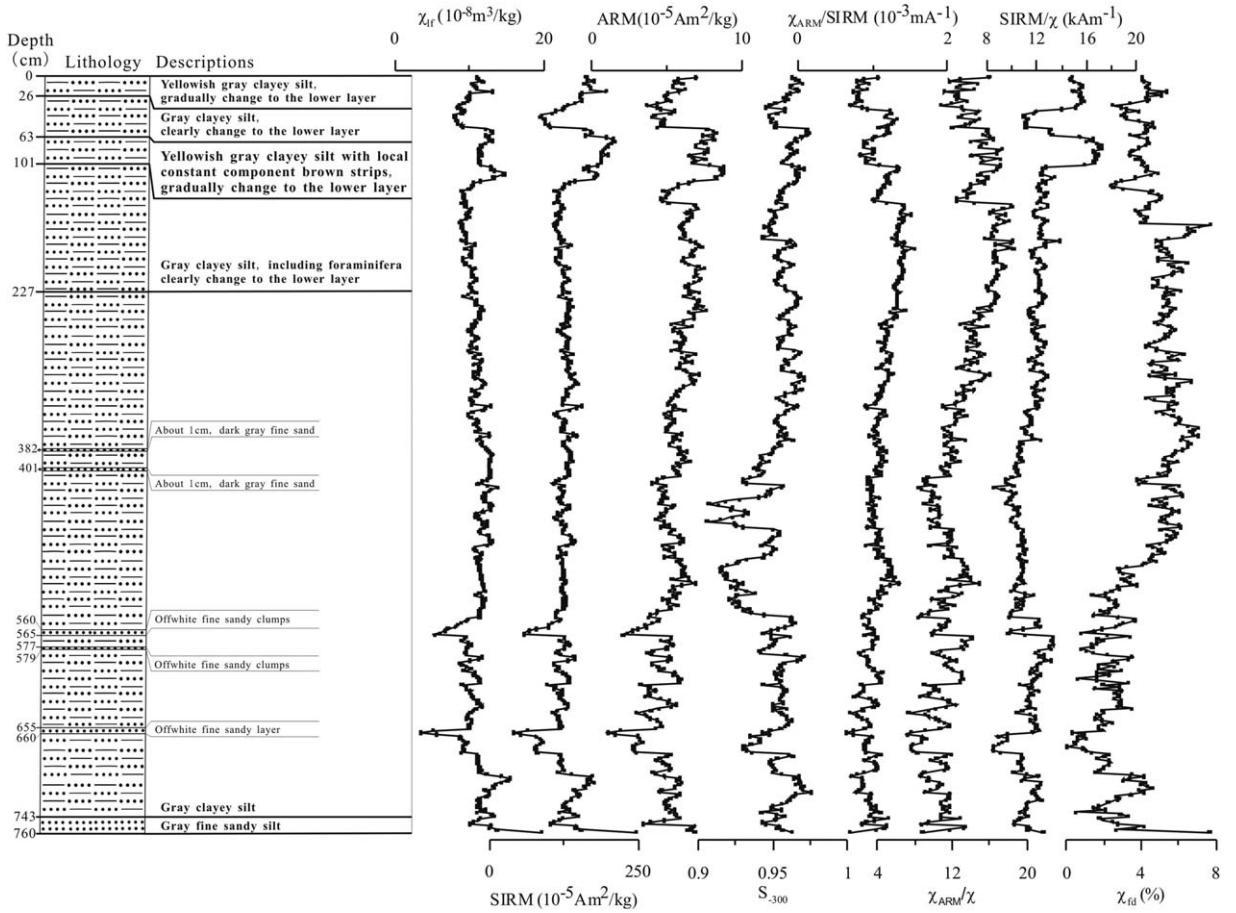

Figure 4. Stratigraphic column and down-core variations of magnetic parameters for samples from core PC24. χ_{lf}, SIRM, and ARM mainly reflect variations in magnetite concentration. S_{-300} reflects variations in the relative contributions of low (dominant) and high-coercivity magnetic minerals [*Bloemendal et al*., 1992]. χ_{ARM}/χ, χ_{ARM}/SIRM, and SIRM/χ and χ_{fd} reflect (minor) variations in magnetite grain size. All magnetic parameters shown are bulk parameters that are widely used in relative paleointensity studies, but do not provide meaningful information when the magnetic mineral assemblage contains mixtures of magnetic minerals or mixed grain size distributions for a single magnetic mineral.

in different ways. The brute force approach is not useful in this context because potentially different signals due to the two magnetite components are unlikely to be discriminated. The "pseudo-Thellier" approach [*Tauxe et al*., 1995] is more useful in the present situation because it enables assessment of the slope of NRM to ARM or IRM over the entire range of applied AF demagnetization fields. As discussed above, we use ARM demagnetization rather than acquisition. The FORC diagrams in Figure 5 contain signals due to noninteracting biogenic magnetite and a detrital magnetite components. The vertical spread of the FORC distributions associated with the detrital component might be interpreted to indicate magnetic interactions that would nullify the assumption of equivalence of ARM acquisition and demagnetization. However, this vertical spread is typical of PSD particle systems [*Roberts et al*., 2000; *Muxworthy and Dunlop*, 2002] and is more likely to be due to magnetization processes within particles rather than among particles [e.g., *Pike et al*., 2001]. We, therefore, treat ARM acquisition and demagnetization data as if they are broadly equivalent in assessing recording of relative paleointensity signals in core PC24.

Linear slopes over the entire range of fields in plots of NRM-ARM demagnetization indicate that the two parameters have similar demagnetization spectra, which is ideal for effective normalization [e.g., *Channell et al*., 2013]. NRM-ARM plots for the studied samples are curved rather than linear (Figure 7a). Curved NRM-ARM plots can result from an individual magnetic component [e.g., *Egli*, 2004] or from mixtures. We assessed the origin of the curved NRM-ARM trends to determine whether they are due to a single magnetic mineral component or to mixtures of detrital and biogenic magnetites. We quantified curvature of NRM-ARM trends using the k parameter of *Paterson* [2011], which is used to assess curvature in Arai diagrams.

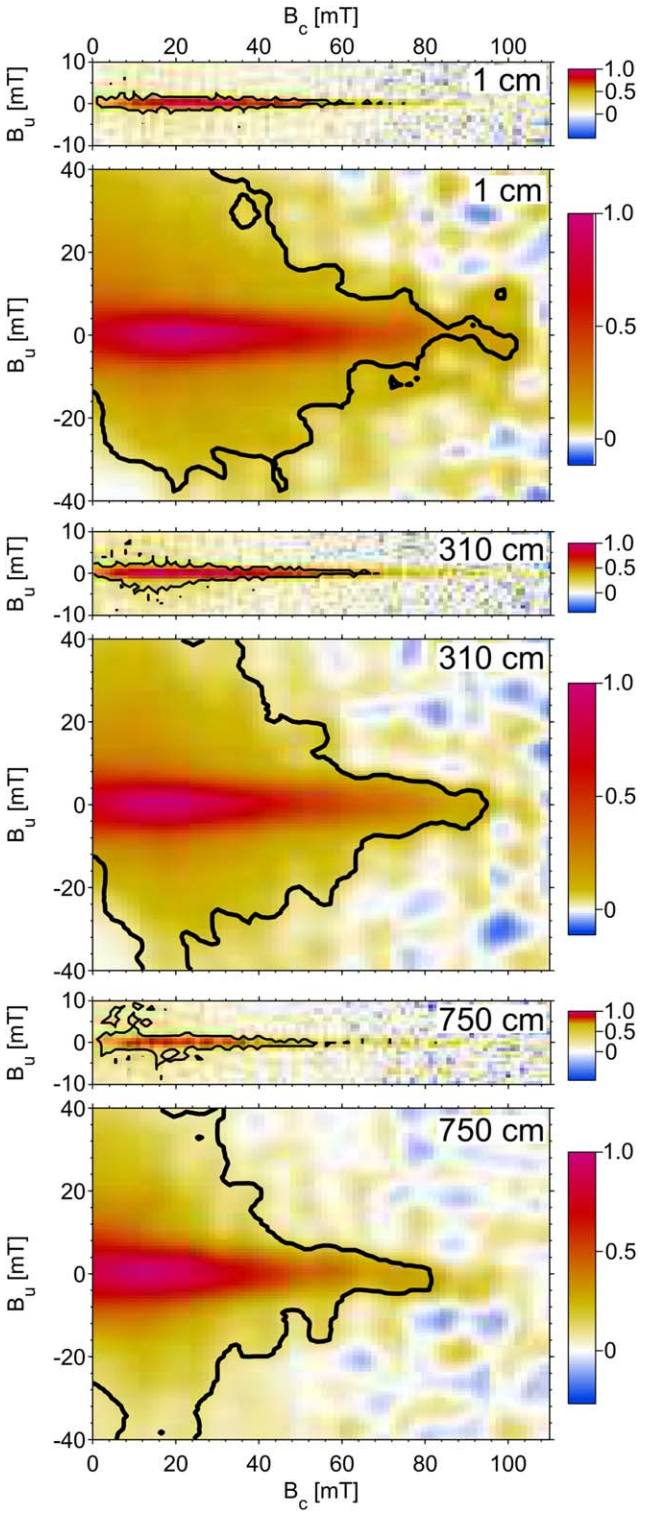

Figure 5. FORC diagrams for representative samples from three depths in core PC24. For each pair of FORC diagrams, the upper diagram represents high-resolution measurements that are designed to resolve the central ridge feature due to intact magnetofossil chains [cf. *Egli et al.*, 2010]. The lower diagrams have lower resolution and enable detection of the detrital PSD contribution [cf. *Roberts et al.*, 2000; *Muxworthy and Dunlop*, 2002]. The dark contour on the FORC diagrams represents the 0.05 significance level, which was calculated according to *Heslop and Roberts* [2012].

This parameter will be zero for a straight line (no curvature) and increases with increasing curvature. $k_{NRM\text{-}ARM}$ is plotted versus the median destructive field of the NRM (MDF_{NRM}) in Figure 7b. As can be seen from the color-coding in Figures 7b and 7c, as the NRM becomes harder (larger MDF_{NRM}), the curvature of NRM-ARM demagnetization plots increases. This indicates that greater NRM-ARM curvature is related to mixing, with higher MDF_{NRM} corresponding to a greater proportion of biogenic magnetite with respect to lower coercivity detrital magnetite. Thus, in conclusion, the curved NRM-ARM trends indicate that the two identified magnetite components have overlapping demagnetization spectra (Figure 7a), with high-coercivity (biogenic) and low-coercivity (detrital) magnetite components having different slopes that will give rise to contrasting paleointensity estimates.

In order to objectively assess the change-point between the overlapping coercivity components represented by different slopes in NRM versus ARM curves, we fitted two separate reduced major axis (RMA) [*Coe et al.*, 1978] lines to the low and high-field demagnetization data. The optimal change-point location (i.e., the field that marks the transition from the low to high-field RMA line) was determined numerically [*Brent*, 1973], with uncertainties estimated using a bootstrap with replacement scheme [*Efron and Tibshirani*, 1993]. On the basis of 1000 bootstraps, 95% of the change-points were found to lie in the interval between the 25 and 30 mT demagnetization steps (Figure 7a). The demagnetization data were, therefore, segmented into low (5–25 mT) and high-field (35–80 mT) sections. Segment specific RMA lines and standard errors [*Coe et al.*, 1978] were then calculated for each sample in the NRM versus ARM, NRM versus IRM, and ARM versus IRM data sets. Demagnetization curves do not typically meet the assumptions of RMA

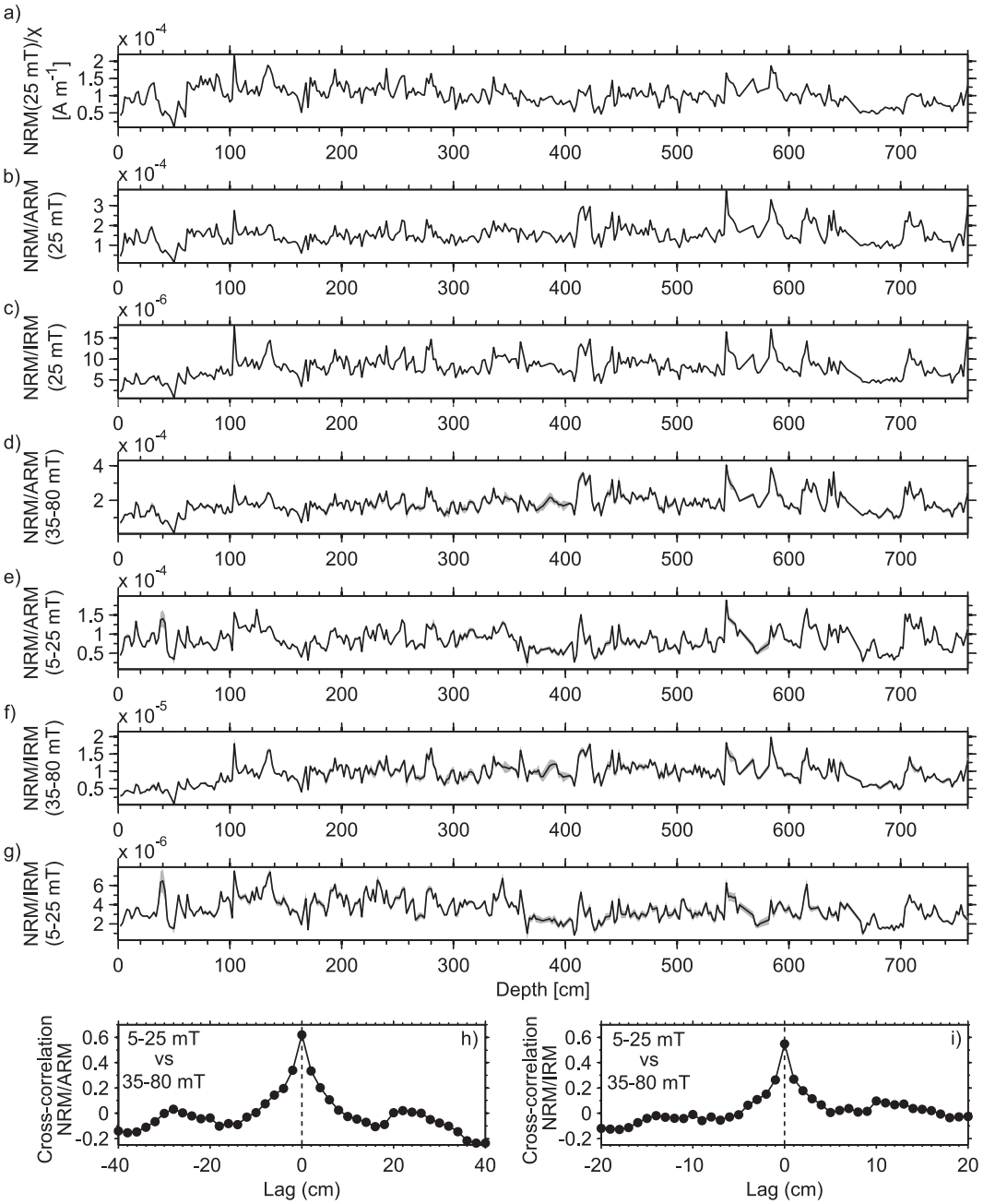

Figure 6. Comparison of (a–c) three "brute force" normalizations used in relative paleointensity investigations, with (d–g) analysis of slopes in NRM-ARM and NRM-IRM demagnetization trends, and (h–i) cross-correlation analysis of the normalized remanence records for normalizations over different demagnetization ranges. (a) NRM/χ, (b) NRM/ARM, and (c) NRM/IRM, all after AF demagnetization at 25 mT. Slope analysis for high (35–80 mT) and low-coercivity (5–25 mT) segments, which correspond to contributions from biogenic and detrital magnetites. (d, e) Slopes of NRM/ARM, and (f, g) NRM/IRM for the biogenic and detrital components, respectively. Standard errors associated with slope determinations are shown with gray shading. (h) Cross correlation for the low and high-coercivity NRM/ARM records. The highest correlation is at zero lag, which indicates that there is no depth offset between the signals. (i) Same as Figure 6h for the low and high-coercivity NRM/IRM records.

line fitting [*Warton et al*., 2006], which supports the statement by *Coe et al*. [1978] that the standard error on the slope cannot be attributed a strict statistical meaning. We, therefore, use the standard error only as a general guide to the uncertainty associated with the estimated RMA slope.

Our approach enables the low and high-field NRM-ARM slopes to be assessed, which can then be used to test how detrital magnetite records paleointensity signals compared to biogenic magnetite

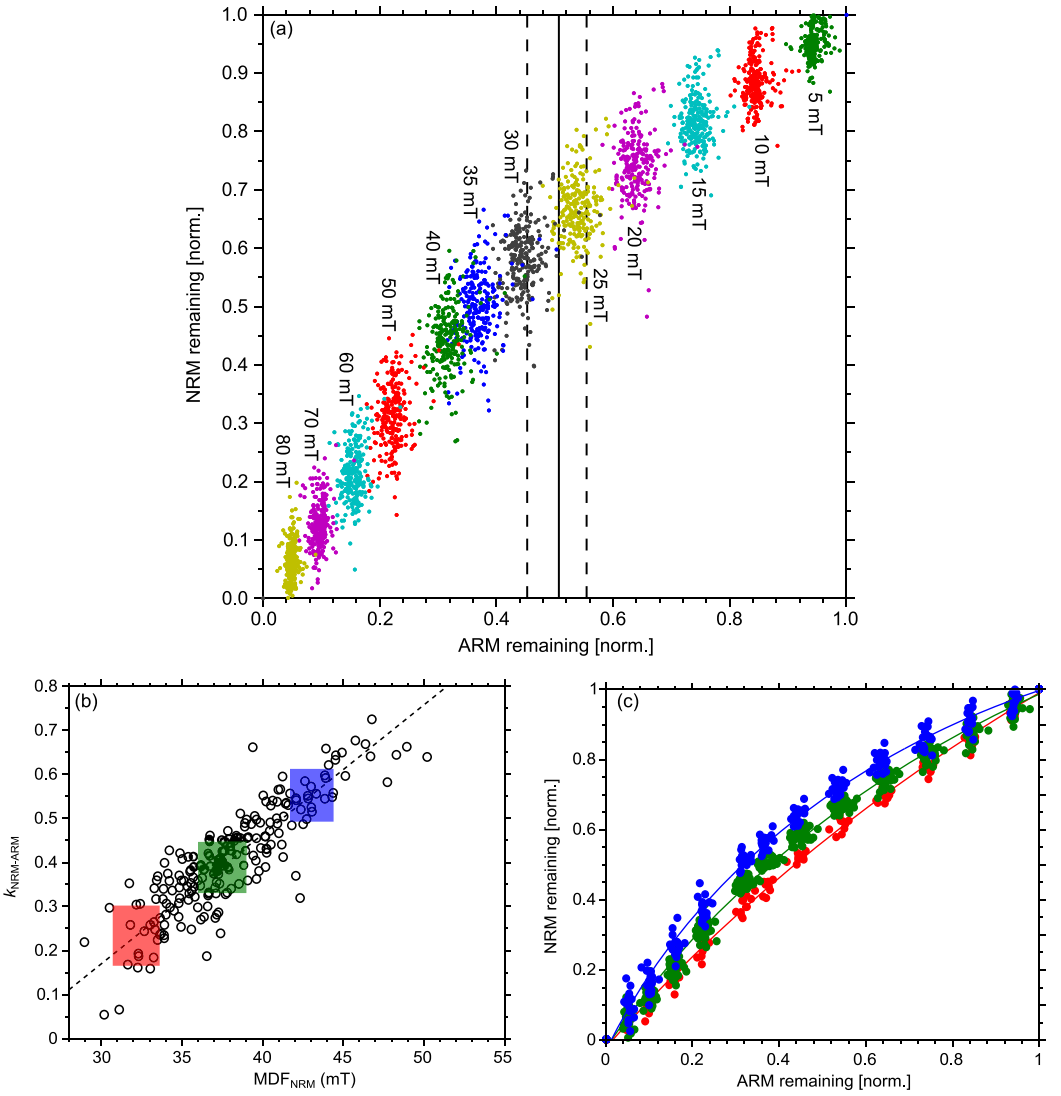

Figure 7. Illustration of the two slopes present when plotting NRM and ARM demagnetization data for samples from core PC24 that exhibited monotonically decreasing NRM intensity (238 samples from a total of 353). In Figure 7a, demagnetization levels are indicated for different colored data clusters. To objectively identify the change-point between slopes, 1000 bootstraps were used; 95% of change-points lie in the interval between the 25 and 30 mT demagnetization steps (vertical solid black line = median, dashed lines = 95th percentiles). Line segments were, therefore, fitted to demagnetization data from each sample for the low (5–25 mT) and high-field (35–80 mT) intervals to provide an estimation of the response of detrital and biogenic particles to the magnetizing field. (b) Plot of the curvature parameter ($k_{NRM-ARM}$) of *Paterson* [2011] for each NRM-ARM curve in Figure 7a versus the median destructive field of the NRM (MDF_{NRM}). $k_{NRM-ARM}$ increases with increasing curvature, with a zero value indicating no curvature (straight line). (c) Illustration of increasing curvature of NRM-ARM plots with increasing proportion of harder biogenic magnetite in mixtures with softer detrital magnetite, where the color-coding is the same as in Figure 7b.

(Figures 6d–6g). The coercivity spectra of the detrital and biogenic magnetites overlap strongly (Figure 3d) and each component will, therefore, contribute to both the low and high-field NRM-ARM slopes. The low-field slope will, however, be dominated by the detrital component, while biogenic magnetite will predominantly control the high-field slope. Thus, while the influence of the detrital and biogenic components cannot be separated completely, such an approach will help to untangle potential differences in the magnetic recording capacity of these two types of magnetite, which have different grain size distributions. As stated above, we do not have a robust age model for core PC24 due to the lack of foraminiferal calcite, so we do not consider our results with respect to age, but restrict our analysis to down-core results and consideration of remanence acquisition efficiency and its implications for paleointensity recording.

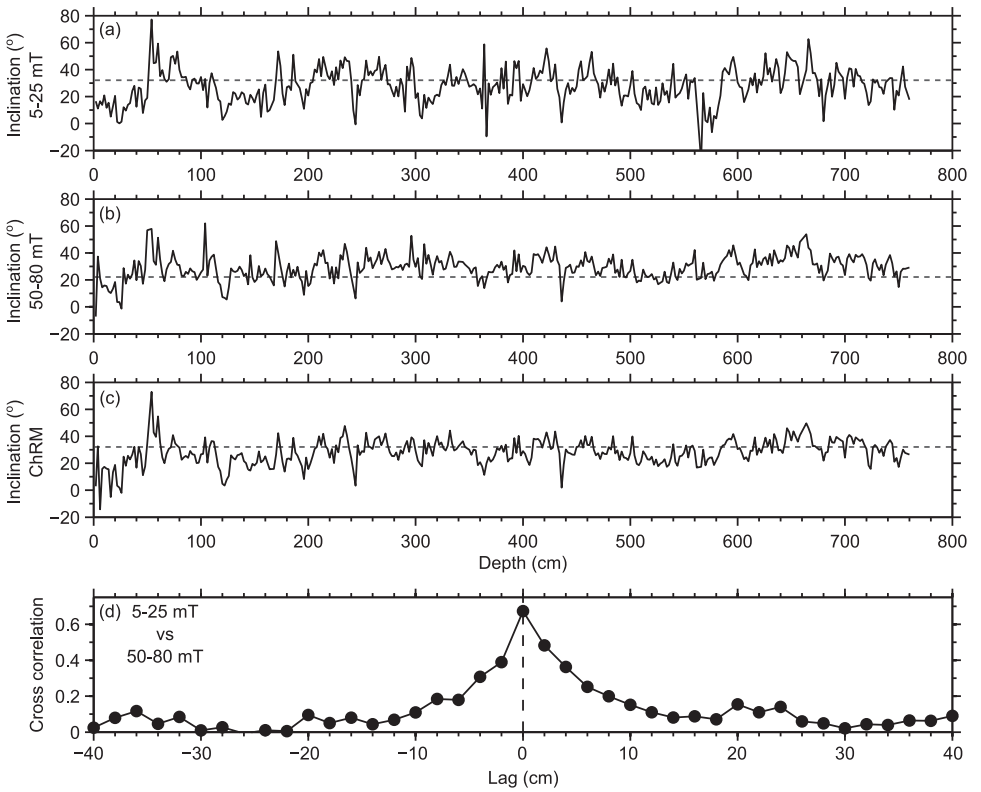

Figure 8. Paleomagnetic inclinations for piston core PC24. The records are after principal component analysis for (a) the 5–25 mT interval (not anchored to the origin of the vector component plots), (b) the 50–80 mT interval (anchored) and for (c) the ChRM (anchored). Gray dashed lines represent the expected geocentric axial dipole field inclination at the site latitude. (d) Cross-correlation results for the low and high-coercivity inclination records. The highest correlation is at zero lag, which indicates that there is no depth offset between paleomagnetic directions carried by the biogenic and detrital magnetite components.

5. Discussion

5.1. Is a Biogeochemical Remanent Magnetization Present in the Studied Sediments?

When considering the relative effects of the combined presence of detrital and biogenic magnetites on remanence acquisition, it is important to consider whether they acquired their respective remanences via different acquisition mechanisms. In particular, it is important to ascertain whether biogenic magnetite carries a biogeochemical remanent magnetization because it will be recorded at greater depth than a DRM or PDRM, so that its paleomagnetic record will be offset from that recorded by detrital magnetite. We test this possibility in two ways. We search for offsets between detrital and biogenic components in (i) our estimations of "relative paleointensity" from NRM-ARM and NRM-IRM slopes, and (ii) paleomagnetic directions. There are no obvious offsets in estimations of "relative paleointensity" for the two components (Figures 6d–6g), which has been confirmed by cross-correlation analysis (Figures 6h–6i). Paleomagnetic directions were determined using principal component analysis for the 5–25 and 50–80 mT intervals and for the ChRM selected from the entire demagnetization range (Figures 8a–8c). Cross-correlation analysis (Figure 8d) indicates that the highest correlation occurs at zero lag so that there are no offsets between the paleomagnetic directions carried by biogenic and detrital magnetites.

Lack of evidence for depth offsets between biogenic and detrital paleomagnetic signals in the studied South China Sea sediments suggests that the magnetotactic bacteria that produced the biogenic magnetite lived and died at sufficiently shallow depths within the sediment column that their inorganic magnetic remains contributed to a paleomagnetic signal that was acquired essentially synchronously with that recorded by detrital magnetite particles. This suggests that, at deepest, the magnetotactic bacteria lived within the surface mixed layer of the sediments [cf. *Mao et al*., 2014]. We, therefore, interpret the recorded biogenic paleomagnetic signal as contributing to a conventional DRM or PDRM rather than to a distinct biogeochemical remanent magnetization [cf. *Tarduno et al*., 1998].

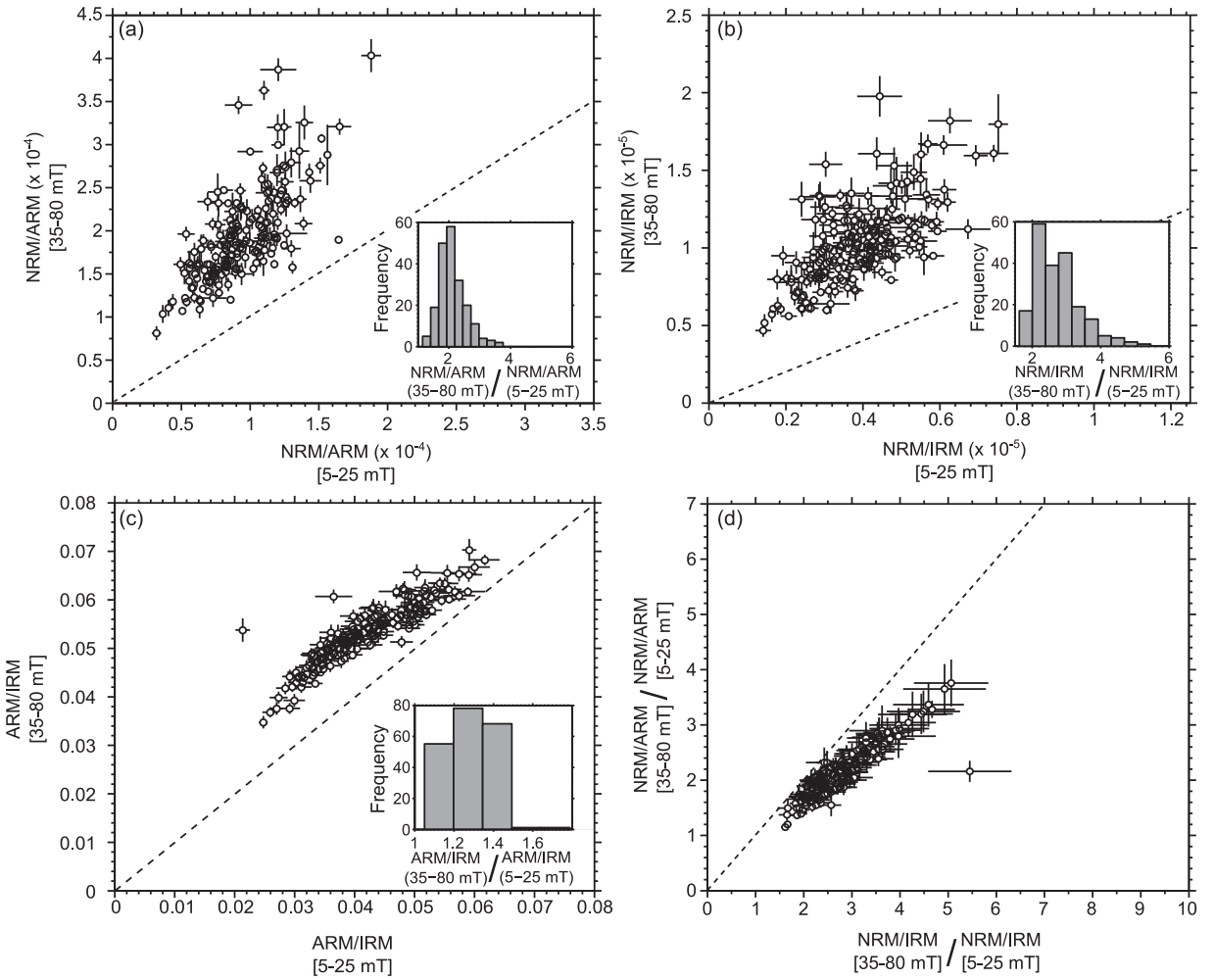

Figure 9. Analysis of the efficiency of remanence acquisition for biogenic and detrital magnetites for samples from core PC24 that exhibited monotonically decreasing NRM intensity during demagnetization. Equivalent remanence acquisition efficiency would be indicated by data falling around the 1:1 slope. (a) NRM/ARM and (b) NRM/IRM for the high coercivity (biogenic) versus the low coercivity (detrital) components. All data fall above the 1:1 line. This suggests that the biogenic component was acquired more efficiently than the detrital component. In histograms of average slopes (insets), biogenic magnetizations are typically more than twice as efficient as detrital magnetizations. (c) The grain-size proxy ratio, ARM/IRM, for the biogenic versus the detrital components. The data lie above the 1:1 line, which suggests preferential acquisition of ARM by biogenic magnetite. This bias can account for Figure 9d the difference in NRM-ARM and NRM-IRM normalizations. However, it does not explain the steeper slopes of both NRM-ARM and NRM-IRM for the biogenic component, which indicates that the biogenic component acquires a remanence more efficiently than the detrital component. Error bars in Figures 9a–9c represent standard errors for the fitted lines (see Figure 6) [*Coe et al*., 1978], while in Figure 9d standard errors were obtained by error propagation (i.e., addition in quadrature of fractional uncertainties [*Taylor*, 1987]).

5.2. Does Biogenic Magnetite Have a Different Remanence Acquisition Efficiency to Detrital Magnetite?

Having determined that there is no depth offset between paleomagnetic signals recorded by biogenic and detrital magnetic mineral fractions within the studied sediments, it becomes important to assess whether these mineral fractions have different remanence acquisition efficiencies. The observed lack of depth offset suggests that any difference in recording efficiency has no detectable influence on paleomagnetic directions (Figure 8). However, any variable remanence acquisition efficiency is likely to strongly affect paleointensity signal recording.

As seen in our NRM-ARM and NRM-IRM slope analysis (Figures 6d–6g), the detrital and biogenic components do not record identical normalized remanence signals. This suggests that paleointensity recording in the studied sediments is more complex than for paleomagnetic directions. Based on the lack of phase lag between the paleomagnetic directional records, it appears that the biogenic and detrital magnetites were magnetized synchronously. Any differences between "paleointensity" signals recorded by the two components will, therefore, result from variable relative efficiency of remanence acquisition. This provides a rare

opportunity to test the efficiency of remanence acquisition, which is normally assumed to be constant for sedimentary sequences subjected to paleointensity investigations [e.g., *Tauxe*, 1993; *Roberts et al*., 2013a]. The efficiency of remanence acquisition can be assessed from the magnitudes of the slopes for the two components in the NRM-ARM and NRM-IRM diagrams (e.g., Figures 9a and 9b). As is evident in Figure 9a, the relative contribution of the biogenic to detrital components to NRM-ARM is variable. Most importantly, as indicated by the ratio of the slope of the biogenic to the detrital components, the biogenic component is generally at least twice as efficient as the detrital component in recording the paleomagnetic signal, with 95% of estimations having efficiencies that range between factors of 1.4 and 3.2 (Figure 9a, inset). For NRM-IRM slopes, the biogenic component also has more efficient acquisition with 95% of estimations having efficiencies that range between factors of 1.9 and 4.5 (Figure 9b, inset).

Recent redeposition experiments involving dead cells of cultured *Magnetospirillum magneticum* strain AMB-1 confirm that magnetotactic bacteria can give rise to an efficient NRM that is linear with applied field in a range of Earth-like (0–120 μT) fields [*Paterson et al*., 2013]. Redeposition experiments of sediments that contain mixed wild-type magnetotactic bacteria also demonstrate that the acquired NRM is proportional to applied field up to 160 μT [*Mao et al*., 2014]. The relative alignment inefficiency of living magnetotactic bacteria within the sedimentary surface mixed layer (1%), along with postmortem flocculation of magnetofossils with other sediment components, will contribute to the inefficient magnetizations observed in sediments [*Mao et al*., 2014]. Despite this inefficiency, *Mao et al*. [2014] argued that magnetofossil chains will record useful relative paleointensities. However, a consequence of the variability in remanence acquisition efficiency that we have documented for detrital and biogenic magnetites is that the NRM will vary in strength in a way that is not controlled by the geomagnetic field. This will complicate efforts to extract meaningful paleointensity signals using both "brute force" and pseudo-Thellier approaches.

A consideration in the above analysis is whether ARM normalization is affected by the fact that ARM is more prone to activating SD biogenic magnetite particles compared to IRM. In Figure 9c, we plot the grain size indicator, ARM/IRM, for the biogenic component (vertical) versus the detrital (horizontal) component. ARM/IRM ratios fall above the 1:1 line, with 95% of values ranging between 1.1 and 1.5, which confirms that ARM is more efficiently activated, typically by 20–40%, within the biogenic component (Figure 9c, inset). The effect of this bias is illustrated in Figure 9d, where overnormalization due to the greater efficiency of ARM acquisition in biogenic magnetite causes deviation away from the 1:1 line for NRM/ARM compared to NRM/IRM. Nevertheless, the effect of preferential ARM acquisition in biogenic magnetite only causes a bias in the normalization; in all cases, the biogenic magnetite component has steeper slopes (i.e., higher remanence acquisition efficiency) than the detrital component for both ARM and IRM normalizations (Figures 9a and 9b).

Recent recognition of the widespread occurrence of biogenic magnetite in the geological record [e.g., *Roberts et al*., 2012] means that variable remanence acquisition efficiency between biogenic and detrital magnetite components should be suspected more often in sedimentary relative paleointensity investigations [e.g., *Yamazaki et al*., 2013]. More work is, therefore, needed to understand sedimentary remanence acquisition, particularly paleointensity signal recording.

6. Conclusions

We have studied a sediment core from the South China Sea that, based on the use of the bulk magnetic parameters generally used in relative paleointensity investigations, has "uniform" magnetic properties that meet the strict criteria applied in such studies. Despite this, the studied sediments contain approximately equal concentrations of detrital and biogenic magnetites. We expect that mixtures of biogenic and detrital magnetites are much more common than has been recognized in the literature, so we assessed the effects of the two distinct magnetite assemblages, with different grain size distributions, on the recorded "relative paleointensity" signal. We separated the contributions from detrital and biogenic magnetites using the presence of two distinct slopes in NRM-ARM and NRM-IRM demagnetization plots. We observe no depth offsets between "paleointensity" features identified for the two components from this approach, or for paleomagnetic directions determined for the detrital and biogenic magnetite components. This suggests that the biogenic magnetite acquired its paleomagnetic signal at an indistinguishable time with respect to the detrital magnetite component. We, therefore, find no evidence for a separate biogeochemical remanent

magnetization [*Tarduno et al*., 1998] in the studied sediment core, which suggests that the magnetization was acquired along with detrital magnetite particles near the base of the uppermost surficial mixed layer of the sediment. While a biogeochemical remanent magnetization could exist in some settings, our study provides a case where biogenic magnetite does not give rise to this type of remanence. This provided an opportunity to test the remanence acquisition efficiency for the two magnetic mineral components because it appears that the two components were magnetized at the same time (i.e., by an apparently identical ambient field).

The identified "relative paleointensity" components due to detrital and biogenic magnetites are not identical. Furthermore, the relative contribution of the two components to the paleomagnetic signal varies with time (see variable slopes in the insets in Figures 9a and 9b), which suggests variable remanence acquisition efficiency throughout the studied core. The biogenic component is generally at least twice as efficiently magnetized as the detrital component. Our approach should be useful for routine unraveling of important complexities in relative paleointensity investigations. However, variable remanence acquisition efficiency, of the type documented in the studied sediment core, indicates that "brute force" normalization and the pseudo-Thellier approach would both be affected because the NRM intensity is controlled to a considerable extent by a nongeomagnetic factor that is normally assumed to be constant in relative paleointensity studies. We also note that if a biogeochemical remanent magnetization had been recorded, it would complicate paleointensity signal recording more than in the case documented here.

Techniques that enable discrimination of different magnetic mineral components, especially mixtures of detrital and biogenic magnetites, need to be applied routinely in relative paleointensity investigations. Such studies have too often used bulk magnetic parameters that do not provide adequate insight into the nature of magnetic mineral components that can cause variable paleomagnetic recording efficiency in sediments, which has not been widely considered in relative paleointensity investigations. Notable exceptions include studies such as that of *Channell et al*. [2013], who, despite documenting the presence of detrital and biogenic magnetites and detrital hematite, reported relative paleointensity results that match well with global paleointensity stacks. Importantly, *Channell et al*. [2013] documented linear pseudo-Thellier results, with straight lines in NRM demagnetization versus ARM acquisition plots with correlation coefficients (r) that generally exceed 0.98 for the 20–60 mT demagnetization/acquisition interval. Such tests provide crucial verification of a relative paleointensity record. Our results demonstrate that the presence of biogenic and detrital magnetites, which are expected to be widespread in the geological record [*Roberts et al*., 2012], can significantly complicate recording and interpretation of paleomagnetic signals. Greater effort is required to understand how sediments become magnetized and to place sedimentary paleointensity analysis on a firmer theoretical and empirical foundation [cf. *Roberts et al*., 2013a].

Acknowledgments

Our work has benefitted from the support of the Australian Research Council (through grants DP120103952 and DP140104544), the National Science Foundation of China (grant 41272384), the National Basic Research Project (grant 2010CB833405), the China Geological Survey Bureau (grant GZH200900504), and the K. C. Wong Education Foundation, Hong Kong. We thank Bruce Moskowitz (Associate Editor), John King, Ramon Egli, and two anonymous reviewers for their critical insights that have improved the work presented here.

References

Abrajevitch, A., and K. Kodama (2009), Biochemical vs. detrital mechanism of remanence acquisition in marine carbonates: A lesson from the K-T boundary interval, *Earth Planet. Sci. Lett.*, *286*, 269–277.

Bloemendal, J., J. W. King, F. R. Hall, and S. J. Doh (1992), Rock magnetism of late Neogene and Pleistocene deep-sea sediments: Relationship to sediment source, diagenetic processes, and sediment lithology, *J. Geophys. Res.*, *97*, 4361–4375.

Brent, R. P. (1973), *Algorithms for Minimization Without Derivatives*, Prentice Hall, Englewood Cliffs, N. J.

Canfield, D. E., and R. A. Berner (1987), Dissolution and pyritization of magnetite in anoxic marine sediments, *Geochim. Cosmochim. Acta*, *51*, 645–659.

Channell, J. E. T., and H. F. Kleiven (2000), Geomagnetic palaeointensities and astrochronological ages for the Matuyama-Brunhes boundary and the boundaries of the Jaramillo Subchron: Palaeomagnetic and oxygen isotope records from ODP Site 983, *Philos. Trans. R. Soc. London A*, *358*, 1027–1047.

Channell, J. E. T., J. S. Stoner, D. A. Hodell, and C. D. Charles (2000), Geomagnetic paleointensity for the last 100 kyr from the sub-Antarctic South Atlantic: A tool for inter-hemispheric correlation, *Earth Planet. Sci. Lett.*, *175*, 145–160.

Channell, J. E. T., C. Xuan, and D. A. Hodell (2009), Stacking paleointensity and oxygen isotope data for the last 1.5 Myr (PISO-1500), *Earth Planet. Sci. Lett.*, *283*, 14–23.

Channell, J. E. T., D. A. Hodell, V. Margari, L. C. Skinner, P. C. Tzedakis, and M. S. Kesler (2013), Biogenic magnetite, detrital hematite, and relative paleointensity in Quaternary sediments from the Southwest Iberian Margin, *Earth Planet. Sci. Lett.*, *376*, 99–109.

Coe, R. S., S. Grommé, and E. A. Mankinen (1978), Geomagnetic paleointensities from radiocarbon-dated lava flows on Hawaii and the question of the Pacific nondipole low, *J. Geophys. Res.*, *8*, 1740–1756.

Day, R., M. Fuller, and V. A. Schmidt (1977), Hysteresis properties of titanomagnetites: Grain-size and compositional dependence, *Phys. Earth Planet. Inter.*, *13*, 260–267.

Deng, C. L., R. X. Zhu, K. L. Verosub, M. J. Singer, and N. J. Vidic, (2004), Mineral magnetic properties of loess/paleosol couplets of the central loess plateau of China over the last 1.2 Myr, *J. Geophys. Res.*, *109*, B01103, doi:10.1029/2003JB002532.

Dunlop, D. J. (2002), Theory and application of the Day plot (M_{rs}/M_s versus H_{cr}/H_c) 2. Application to data for rocks, sediments, and soils, *J. Geophys. Res.*, *107*(B3), 2056, doi:10.1029/2001JB000487.

Efron, B., and R. J. Tibshirani (1993), *An Introduction to the Bootstrap*, Chapman and Hall, N. Y.

Egli, R. (2004), Characterization of individual rock magnetic components by analysis of remanence curves, 1. Unmixing natural sediments, *Stud. Geophys. Geod.*, *48*, 391–446.
Egli, R., A. P. Chen, M. Winklhofer, K. P. Kodama, and C. S. Horng (2010), Detection of noninteracting single domain particles using first-order reversal curve diagrams, *Geochem. Geophys. Geosyst.*, *11*, Q01Z11, doi:10.1029/2009GC002916.
Evans, M. E., and F. Heller (2003), *Environmental Magnetism: Principles and Application of Enviromagnetics*, Academic, San Diego.
Flies, C. B., H. M. Jonkers, D. de Beer, K. Bosselmann, M. E. Böttcher, and D. Schüler (2005), Diversity and vertical distribution of magnetotactic bacteria along chemical gradients in freshwater microcosms, *FEMS Microbiol. Ecol.*, *52*, 185–195.
He, L. S., and B. Y. Chen (1987), *The Tectonic Map, The South China Sea Geological and Geophysical Atlas*, Guangdong Cartogr. Press, Guangzhou, Guangdong, China.
Heslop, D., and A. P. Roberts (2012), Estimation of significance levels and confidence intervals for first-order reversal curve distributions, *Geochem. Geophys. Geosyst.*, *13*, Q12Z40, doi:10.1029/2012GC004115.
Jogler, C., et al. (2010), Cultivation-independent characterization of '*Canditatus* Magnetobacterium Bavaricum' via ultrastructural, geochemical, ecological, and metagenomic methods, *Environ. Microbiol.*, *12*, 2466–2478.
Karlin, R., and S. Levi (1983), Diagenesis of magnetic minerals in recent haemipelagic sediments, *Nature*, *303*, 327–330.
King, J., S. K. Banerjee, J. Marvin, and Ö. Özdemir (1982), A comparison of different magnetic methods of determining the relative grain size of magnetite in natural materials: Some results from lake sediments, *Earth Planet. Sci. Lett.*, *59*, 404–419.
King, J. W., S. K. Banerjee, and J. Marvin (1983), A new rock-magnetic approach to selecting sediments for geomagnetic paleointensity studies: Application to paleointensity for the last 4000 years, *J. Geophys. Res.*, *88*, 5911–5921.
Kirschvink, J. L. (1980), The least-squares line and plane and the analysis of palaeomagnetic data, *Geophys. J. R. Astron. Soc.*, *62*, 699–718.
Kruiver, P. P., M. J. Dekkers, and D. Heslop (2001), Quantification of magnetic coercivity components by the analysis of acquisition curves of isothermal remanent magnetization, *Earth Planet. Sci. Lett.*, *189*, 269–276.
Laj, C., C. Kissel, A. Mazaud, J. E. T. Channell, and J. Beer (2000), North Atlantic palaeointensity stack since 75ka (NAPIS-75) and the duration of the Laschamp event, *Philos. Trans. R. Soc. London A*, *358*, 1009–1025.
Laj, C., C. Kissel, and A. P. Roberts (2006), Geomagnetic field behavior during the Iceland Basin and Laschamp geomagnetic excursions: A simple transitional field geometry?, *Geochem. Geophys. Geosyst.*, *7*, Q03004, doi:10.1029/2005GC001122.
Larrasoaña, J. C., Q. Liu, P. Hu, P. Mata, J. N. Pérez-Asensio, J. Civis, and A. P. Roberts (2014), Paleomagnetic and paleoenvironmental implications of magnetofossils in late Miocene marine sediments from the Guadalquivir Basin (SW Spain), *Frontiers Microbiol.*, *5*, 71, doi: 10.3389/fmicb.2014.00071.
Levi, S., and S. Banerjee (1976), On the possibility of obtaining relative paleointensities from lake sediments, *Earth Planet. Sci. Lett.*, *29*, 219–226.
Liu, G. D. (Ed.) (1992), *The Geological and Geophysical Map of the China's Seas and Adjacent Areas (at Scale of 1:5 million)*, Geol. Publ. House, Beijing.
Lyle, M. (1983), The brown-green color transition in marine sediments: A marker of the Fe(III)-Fe(II) redox boundary, *Limnol. Oceanogr.*, *28*, 1026–1033.
Mao, X., R. Egli, N. Petersen, M. Hanzlik, and X. Zhao (2014), Magnetotaxis and acquisition of detrital remanent magnetization by magnetotactic bacteria in natural sediment: First experimental results and theory, *Geochem. Geophys. Geosyst.*, *15*, 255–283, doi:10.1002/2013GC005034.
Miao, Q. M., R. C. Thunell, and D. M. Anderson (1994), Glacial-Holocene carbonate dissolution and sea surface temperatures in the South China and Sulu Seas, *Paleoceanography*, *9*, 269–290.
Muxworthy, A. R., and D. J. Dunlop (2002), First-order reversal curve (FORC) diagrams for pseudo-single-domain magnetites at high temperature, *Earth Planet. Sci. Lett.*, *203*, 369–382.
Nagata, T., Y. Arai, and K. Momose (1963), Secular variation of the geomagnetic total force during the last 5000 years, *J. Geophys. Res.*, *68*, 5277–5282.
Ohneiser, C., G. Acton, J. E. T. Channell, G. S. Wilson, Y. Yamamoto, and T. Yamazaki (2013), A middle Miocene relative paleointensity record from the Equatorial Pacific, *Earth Planet. Sci. Lett.*, *374*, 227–238.
Pan, Y. X., N. Petersen, A. F. Davila, L. Zhang, M. Winklhofer, Q. S. Liu, M. Hanzlik, and R. X. Zhu (2005), The detection of bacterial magnetite in recent sediments of Lake Chiemsee, *Earth Planet. Sci. Lett.*, *237*, 109–123.
Paterson, G. A. (2011), A simple test for the presence of multidomain behavior during paleointensity experiments, *J. Geophys. Res.*, *116*, B10104, doi:10.1029/2011JB008369.
Paterson, G. A., Y. Wang, and Y. Pan (2013), The fidelity of paleomagnetic records carried by magnetosome chains, *Earth Planet. Sci. Lett.*, *383*, 82–91.
Petermann, H., and U. Bleil (1993), Detection of live magnetotactic bacteria in South Atlantic deep-sea sediments, *Earth Planet. Sci. Lett.*, *117*, 223–228.
Pike, C. R., A. P. Roberts, M. J. Dekkers, and K. L. Verosub (2001), An investigation of multi-domain hysteresis mechanisms using FORC diagrams, *Phys. Earth Planet. Inter.*, *126*, 11–25.
Roberts, A. P., C. R. Pike, and K. L. Verosub (2000), First-order reversal curve diagrams: A new tool for characterizing the magnetic properties of natural samples, *J. Geophys. Res.*, *105*, 28,461–28,475.
Roberts, A. P., L. Chang, D. Heslop, F. Florindo, and J. C. Larrasoaña (2012), Searching for single domain magnetite in the 'pseudo-single-domain' sedimentary haystack: Implications of biogenic magnetite preservation for sediment magnetism and relative paleointensity determinations, *J. Geophys. Res.*, *117*, B08104, doi:10.1029/2012JB009412.
Roberts, A. P., L. Tauxe, and D. Heslop (2013a), Magnetic paleointensity stratigraphy and high-resolution Quaternary geochronology: Successes and future challenges, *Quat. Sci. Rev.*, *61*, 1–16.
Roberts, A. P., F. Florindo, L. Chang, D. Heslop, L. Jovane, and J. C. Larrasoaña (2013b), Magnetic properties of pelagic marine carbonates, *Earth Sci. Rev.*, *127*, 111–139.
Rottman, M. L. (1979), Dissolution of planktonic foraminifera and pteropods in the South China Sea sediments, *J. Foraminiferal Res.*, *9*, 41–49.
Stoner, J. S., C. Laj, J. E. T. Channell, and C. Kissel (2002), South Atlantic and North Atlantic geomagnetic paleointensity stacks (0–80 ka): Implications for inter-hemispheric correlation, *Quat. Sci. Rev.*, *21*, 1141–1151.
Tauxe, L. (1993), Sedimentary records of relative paleointensity of the geomagnetic field: Theory and practice, *Rev. Geophys.*, *31*, 319–354.
Tauxe, L., and T. Yamazaki (2007), Paleointensities, in *Treatise on Geophysics*, vol. 5, *Geomagnetism*, edited by G. Schubert, pp. 509–564, Elsevier, Oxford, U. K.
Tauxe, L., T. Pick, and Y. S. Kok (1995), Relative paleointensity in sediments: A pseudo-Thellier approach, *Geophys. Res. Lett.*, *22*, 2885–2888.

Tauxe, L., J. L. Steindorf, and A. Harris (2006), Depositional remanent magnetization: Toward an improved theoretical and experimental foundation, *Earth Planet. Sci. Lett.*, *244*, 515–529.
Tarduno, J. A., W. L. Tian, and S. Wilkison (1998), Biogeochemical remanent magnetization in pelagic sediments of the western equatorial Pacific Ocean, *Geophys. Res. Lett.*, *25*, 3987–3990.
Taylor, J. R. (1987), *An Introduction to Error Analysis: The Study of Uncertainties in Physical Measurements*, Univ. Sci. Books, Berkeley, Calif.
Thompson, R., and F. Oldfield (1986), *Environmental Magnetism*, Allen and Unwin, London.
Thellier, E., and O. Thellier (1959), Sur l'intensité du champ magnétique terrestre dans la passé historique et géologique, *Ann. Geophys.*, *15*, 285–376.
Thunell, R. C., Q. M. Miao, S. E. Calvert, and T. F. Pedersen (1992), Glacial-Holocene biogenic sedimentation patterns in the South China Sea: Productivity variations and surface water pCO_2, *Paleoceanography*, *7*, 143–162.
Valet, J. P. (2003), Time variations in geomagnetic intensity, *Rev. Geophys.*, *41*, 1004, doi:10.1029/2001RG000104.
Valet, J. P., L. Meynadier, and Y. Guyodo (2005), Geomagnetic dipole strength and reversal rate over the past two million years, *Nature*, *435*, 802–805.
Verosub, K. L., and A. P. Roberts (1995), Environmental magnetism: Past, present, and future, *J. Geophys. Res.*, *100*, 2175–2192.
Wang, P. X., L. J. Wang, Y. H. Bian, and Z. M. Jian (1995), Late Quaternary paleoceanography of the South China Sea: Surface circulation and carbonate cycles, *Mar. Geol.*, *127*, 145–165.
Warton, D. I., I. J. Wright, D. S. Falster, and M. Westoby (2006), Bivariate line-fitting methods for allometry, *Biol. Rev.*, *81*, 259–291.
Wei, K. Y., T. N. Yang, and C. Y. Huang (1997), Glacial Holocene calcareous nannofossils and paleoceanography in the northern South China Sea, *Mar. Micropaleontol.*, *32*, 95–114.
Yamazaki, T., and P. Sølheid (2011), Maghemite-to-magnetite reduction across the Fe-redox boundary in a sediment core from the Ontong-Java Plateau: Influence on relative palaeointensity estimation and environmental magnetic application, *Geophys. J. Int.*, *185*, 1243–1254, doi:10.1111/j.1365-246X.2011.05021.x.
Yamazaki, T., Y. Yamamoto, G. Acton, E. P. Guidry, and C. Richter (2013), Rock-magnetic artifacts on long-term relative paleointensity variations in sediments, *Geochem. Geophys. Geosyst.*, *14*, 29–43, doi:10.1029/2012GC004546.
Yang, X. Q., W. J. Zhou, F. L. Gao, and H. M. Li (2007), Remanence magnetic records of the recent 130000 years from the sediments in Nansha area, South China Sea, *Front. Earth Sci. China*, *1*, 80–87.
Yang, X. Q., F. Heller, N. Y. Wu, J. Yang, and Z. H. Su (2009), Geomagnetic paleointensity dating of South China Sea sediments for the last 130 kyr, *Earth Planet. Sci. Lett.*, *284*, 258–266.
Zhang, C. X., G. A. Paterson, and Q. S. Liu (2012), A new mechanism for the magnetic enhancement of hematite during heating: The role of clay minerals, *Stud. Geophys. Geod.*, *56*, 845–860.
Ziegler, L. B., C. G. Constable, C. L. Johnson, and L. Tauxe (2011), PADM2M: A penalized maximum likelihood model of the 0–2 Ma palaeomagnetic axial dipole moment, *Geophys. J. Int.*, *184*, 1069–1089.